Molecular Microbiology (2006) **61**(2), 394–406
doi:10.1111/j.1365-2958.2006.05246.x
First published online 12 June 2006

Differential modulation of *E. coli* mRNA abundance by inhibitory proteins that alter the composition of the degradosome

Junjun Gao,[1‡] Kangseok Lee,[2†‡] Meng Zhao,[1] Ji Qiu,[1,4] Xiaoming Zhan,[1,4] Ankur Saxena,[4] Christopher J. Moore,[2] Stanley N. Cohen[2,3] and George Georgiou[1,4,5*]

[1]*Institute for Cell and Molecular Biology,* [4]*Departments of Chemical Engineering and* [5]*Biomedical Engineering, University of Texas, Austin, TX 78712, USA.*

[2]*Departments of Genetics and* [3]*Medicine, Stanford University School of Medicine, Stanford, CA 94305, USA.*

Summary

In *Escherichia coli* the initial step in the processing or decay of many messenger and structural RNAs is mediated by the endonuclease RNase E, which forms the core of a large RNA-catalysis machine termed the degradosome. Previous experiments have identified a protein that globally modulates RNA abundance by binding to RNase E and regulating its endonucleolytic activity. Here we report the discovery of RraB, which interacts with a different site on RNase E and interferes with cleavage of a different set of transcripts. We show that expression of RraA or RraB *in vivo* is accompanied by dramatic, distinct, and inhibitor-specific changes in degradosome composition – and that these are in turn associated with alterations in RNA decay and global transcript abundance profiles that are dissimilar to the profile observed during simple RNase E deficiency. Our results reveal the existence of endonuclease binding proteins that modulate the remodelling of degradosome composition in bacteria and argue that such degradosome remodelling is a mechanism for the differential regulation of RNA cleavages in *E. coli*.

Introduction

The multifaceted actions of endoribonuclease RNase E in RNA metabolism include the processing of ribosomal and tRNAs, the turnover of numerous cellular mRNAs, and the degradation of small regulatory RNAs (e.g. Ghora and Apirion, 1978; Li *et al*., 1999; Lin-Chao *et al*., 1999; Bernstein *et al*., 2002; Li and Deutscher, 2002; Masse *et al*., 2003; for review, see Steege, 2000; Kushner, 2002). This essential 118 kDa enzyme contains 1061 amino acids that can be grouped into at least three distinct domains (Cohen and McDowall, 1997). The first 500 amino acids at the amino terminal-end of the protein include an endonucleolytically active site (McDowall and Cohen, 1996), which recently has been proposed to be located at or near amino-terminus residues 303–305 (Callaghan *et al*., 2005). The remainder of the protein, termed the C-Terminal half (CTH), consists of an arginine-rich motif with a putative RNA binding site (ARRBS, amino acids 604–688) (Taraseviciene *et al*., 1995; McDowall and Cohen, 1996; Kushner, 2002) and a scaffold region (amino acids 734–1061) that contains binding sites for PNPase, the RhlB RNA helicase, and the glycolytic enzyme enolase (Py *et al*., 1994; 1996; Miczak *et al*., 1996; Vanzo *et al*., 1998; Coburn and Mackie, 1999). Together, RNase E and its associated proteins constitute the major components of a large protein complex termed the degradosome (Carpousis *et al*., 1994; Py *et al*., 1994). Recent studies indicate that the functions of all four major degradosome proteins are required for normal RNA decay and further suggest that components of the assembled degradosome complex work in concert to regulate the degradation of some, but not all, mRNAs in *Escherichia coli* (Bernstein *et al*., 2004; Khemici and Carpousis, 2004). Nonetheless, the CTH is not required for cell survival (Kido *et al*., 1996; Ow *et al*., 2000).

The cellular level and activity of RNase E in *E. coli* are subject to complex control. First, RNase E autoregulates its synthesis by modulating decay of its own mRNA, thus maintaining the enzyme expression at a relatively stable level (Mudd and Higgins, 1993; Jain and Belasco, 1995). Second, 5′ monophosphorylated RNA serves as an allosteric activator of the endonuclease activity (Mackie, 1998; Jiang and Belasco, 2004). Third, RNA decay can be regulated by interaction with RraA (*r*egulator of *r*ibonuclease *a*ctivity A), which inhibits RNase E endonucleolytic cleavages (Lee *et al*., 2003). Elevated expression of RraA, which has been found by structural analysis to form a ring-like trimer with a central cavity of approximately 12 Å

Accepted 15 May, 2006. *For correspondence. E-mail georgiou@che.utexas.edu; Tel. (+1) 512 471 6975; Fax (+1) 512 471 7963. †Present address: Department of Life Science, Chung-Ang University, Seoul, Korea. ‡These authors contributed equally to this work and are listed alphabetically.

in diameter (Monzingo *et al*., 2003), circumvents the effects of the autoregulatory mechanism and modulates the accumulation of over 2000 RNase E-targeted transcripts (Lee *et al*., 2003).

Using a genetic screen that takes advantage of the high sensitivity of mRNA encoded by the disulphide isomerase (*dsbC*) gene to the action of RNase E, we sought to identify additional *E. coli* protein modulators of RNase activity *in vivo*. We report the genetic discovery of a second protein modulator, previously annotated as YjgD in the NCBI database and here renamed RraB, which can – like RraA – inhibit RNase E activity *in vitro* and *in vivo* by binding to the enzyme. Importantly, we show that RraA and RraB interact with RNase E at separate sites within the RNase E and exert dramatic and distinct effects on the composition of the degradosome. The combined action of the two proteins differentially alters mRNA decay in a transcript-specific manner. Our results point to a novel mechanism for the global control of steady-state mRNA abundance in *E. coli* that appears to be mediated by dynamic remodelling of the degradosome composition in response to elevated expression of RraA or RraB.

Results

Transcript-specific inhibition of the endonuclease activity of RNase E by RraB

RraB was identified on the basis of its effect on the abundance of the bacterial disulphide isomerase DsbC, using the same genetic approach employed earlier to isolate RraA (Lee *et al*., 2003). Briefly, an *E. coli* genomic DNA library cloned into the expression vector pTrc99A downstream from the IPTG-inducible Trc promoter, was screened for ability to confer increased folding yield of the multidisulphide reporter protein v-tPA (a truncated human tissue plasminogen activator variant) whose enzymatic activity can be detected via the formation of a clearance zone on fibrin plates. A high v-tPA activity, and hence a large clearance zone, hinges on elevated expression of the disulphide isomerase DsbC, a protein encoded by a RNase E-cleavable transcript with a short half-life (Zhan *et al*., 2004). This screen yielded, in addition to RraA (Lee *et al*., 2003), a clone encoding a single open reading frame (ORF) that corresponds to the hypothetical gene, *yjgD.* The *yjgD* ORF consists of 417 bp and is located at 96.4 min in the *E. coli* chromosome. Because the polypeptide product of this gene was found to serve as a regulator of RNase E activity (see below), we renamed it *rraB* (*r*egulator of *r*ibonuclease *a*ctivity B). RT-PCR and Northern blot analysis confirmed that *rraB* is expressed from its chromosomal copy throughout exponential and stationary phase growth (M.Z., Y. Kawarasaki and G.G., data not shown). *rraB* was subcloned into the expression vector pTrc99A downstream of the IPTG-inducible Trc promoter. Lysates from cells expressing the v-tPA reporter protein (see *Experimental procedures*) with or without RraB were spotted on fibrin plates. As expected, coexpression of RraB resulted in markedly increased fibrinolytic activity, consistent with a higher yield of folded v-tPA (Fig. 1A). In turn, Western blot analysis revealed an elevated cellular level of DsbC protein (Fig. 1B).

As was observed for RraA (Lee *et al*., 2003), RraB expression from a multicopy plasmid resulted in dramatic stabilization of *dsbC* mRNA, increasing its half-life from 95 s to over 300 s (Fig. 2A). Additionally, adventitious expression of RraB conferred an increase in the cellular activity of β-galactosidase encoded by a chromosomal fusion of the *rne* gene with *lacZ* (Jain and Belasco, 1995; Lee *et al*., 2003) (Fig. 2B), suggesting that RraB, like RraA (Jain and Belasco, 1995; Lee *et al*., 2003), can alter the action of RNase E. Further analysis indicated that the observed increase in β-galactosidase activity resulted from decreased RNase E cleavage of the fusion transcript (Fig. 2C), which previously had been shown to occur in the 5′ UTR segment of the *rne*-encoded segment (Mudd

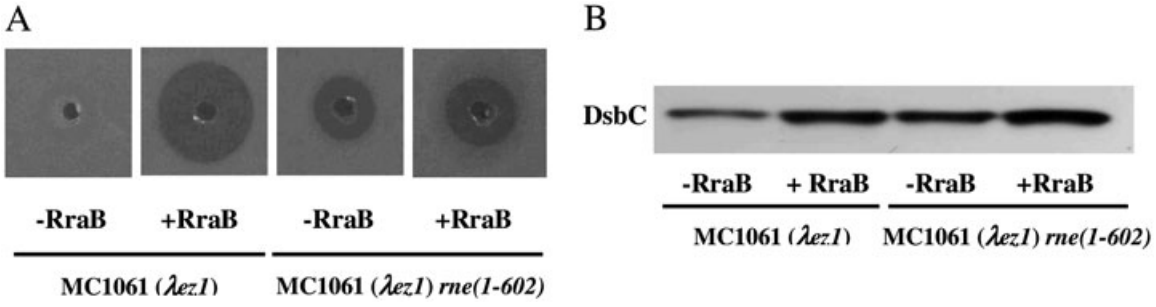

Fig. 1. RraB enhances disulphide isomerization activity by increasing the steady level of DsbC.
A. v-tPA fibrinolytic activity in cell lysates with and without RraB coexpression. Cells were grown to mid-exponential phase in LB media at 37°C and induced with 0.5 mM IPTG. Harvested cells were lysed by French press and 15 μg of total cell lysate protein was spotted on fibrin plates. Clearance zones after 24 h are shown.
B. Western blot analysis of DsbC levels in cell lysate prepared with the same procedure as (A). Equal amount of total cell protein was loaded in each lane.

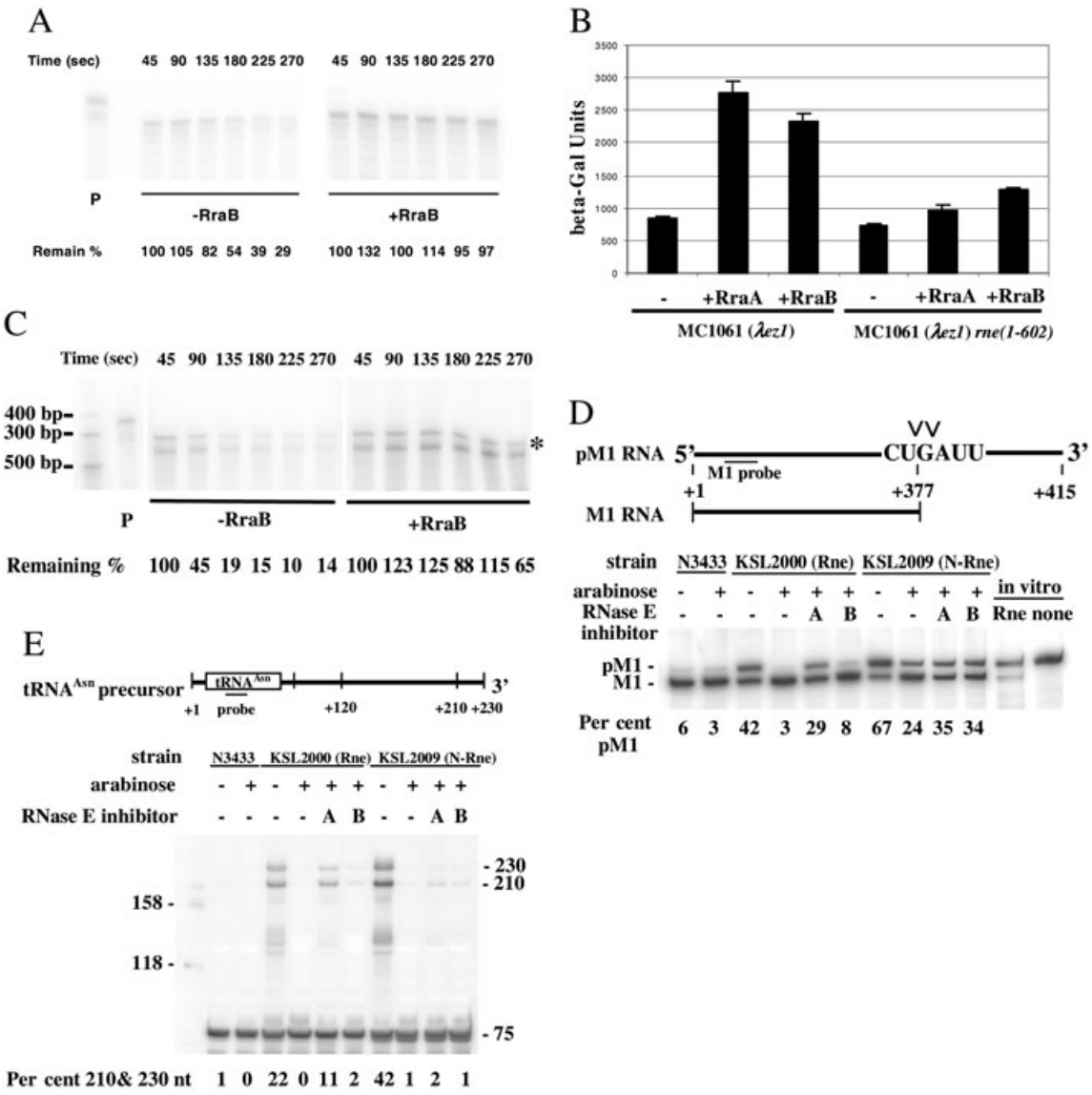

Fig. 2. Inhibition of RNase E activity by RraB is substrate-specific.
A. *dsbC* mRNA decay. Cells were induced with 0.5 mM IPTG and 90 min after induction, rifampicin was added to stop transcription. One millilitre aliquots were collected every 45 s, RNA was extracted and 5 μg of total RNA was used for RNase protection assay. The percentage of remaining *dsbC* mRNA at each time point is calculated by dividing with the signal intensity of the first lane (45 s sample). The experiment was carried out in triplicate and the variation in the $t_{1/2}$-values between repetitions was < 5%. **P**, free probe containing sequence complementary to the +1 to +266 bp of *dsbC* transcript.
B. β-Galactosidase activity expressed from a chromosomal *rne:lacZ* fusion and measured according to the procedure of Miller (1992). Cells transformed with pTrc99A, pTrc-RraA or pTrc-RraB were grown in LB media and induced at A_{600} ~0.2. After 1.5 h induction, the cells were harvested and assayed for β-galactosidase activity. The β-galactosidase activity shown is the average of data from three independent experiments.
C. *rne* 5′ UTR decay. The half-life of the 5′ UTR *rne* of was determined essentially as in (A). Percentage of remaining *rne* 5′ UTR at each time point was calculated by dividing with the signal intensity of the first lane (45 s sample). **P**, free probe containing sequence complementary to the –360 to +33 region of *rne* transcript. Asterisks (*) indicate the position of *rne* 5′ UTR transcript.
D. Processing of pM1. Total RNA was isolated from KSL2000, KSL2009, and their parental strain N3433 overexpressing RraA (A), RraB (B) or no protein (–) from pTrc99A-derived plasmid and separated by 6% PAGE containing 8 M urea. Separated RNA bands were transferred to a Nylon membrane and probed with ^{32}P end-labelled oligo complementary to M1 sequence. Ten nanograms of *in vitro* synthesized pM1 transcript (**none**) and its cleavage products by RNase E (**Rne**) were loaded in the last two lanes as size markers. Percentage pM1 RNA represents the ratio of pM1 to the sum of pM1 and M1 bands hybridized to the probe.
E. Processing of $tRNA^{Asn}$. Same procedure as described in (B) was used except that the total RNA was separated by 8% PAGE containing 8 M urea and probed with an asn-tRNA-specific probe. Per cent 210&230 represents percentage ratio of the sum of the 210 and 230 nt bands to the sum of 75, 210 and 230 nt bands hybridized to the probe. The per cent inhibition was determined by subtracting 15% from the amount of p23 remaining in the presence of inhibitor protein. In the absence of inhibitor protein, 15% of p23 remained intact. In (D) and (E) representative data are shown for one of three triplicates performed with total RNA isolated from different cultures.

and Higgins, 1993; Jain and Belasco, 1995). The effect of RraB on the processing of the *rne* 5′ UTR was statistically indistinguishable from that conferred by RraA expressed from an identical plasmid. Examination of the processing kinetics of the *rne* 5′ UTR revealed that cleavage was inhibited in cells expressing RraB with the $t_{1/2}$ increasing from 90 s to over 225 s (Fig. 2C).

Strain CJ1825/BZ99 contains a truncated version of the *rne* gene encoding a protein that consists only of the catalytic, N-terminal domain of the enzyme (amino acids 1–602) and additionally contains the *rne–lacZ* fusion described above. Expression of RraB in this strain resulted in a modest increase in β-galactosidase activity (Fig. 2B). Further, in contrast to cells synthesizing full-length RNase E, the effect of RraB on the steady-state level of the DsbC protein was not statistically significant (Fig. 1B).

While the above results argue strongly that RraB, like RraA, is an inhibitor of RNase E activity, examination of the steady-state level of a variety of RNAs indicated that RraA and RraB differentially affect the ability of RNase E to attack different substrates. In these experiments, we used *E. coli* strain KSL2000 in which the chromosomal *rne* gene had been inactivated and RNase E instead is synthesized from a plasmid-borne *rne* gene lacking the 5′ UTR (Lee *et al*., 2002) in order to circumvent RNase E cleavage of its own transcript. As protein synthesis from the plasmid is under the control of an arabinose-inducible pBAD promoter, the cellular level of RNase E is determined exclusively by the concentration of arabinose.

pM1, a 415 nt RNA is cleaved at sites near the 3′ end by RNase E to give rise to M1, the 377 nt catalytic component of the tRNA processing ribozyme RNase P (Lundberg and Altman, 1995). KSL2000 cells transformed with pTrc-RraA or pTrc-RraB were grown in the presence of arabinose. Expression of RraA or RraB was induced by the addition of 0.5 mM IPTG and the steady-state levels of the pM1 RNA and asn-tRNA were determined. SDS-PAGE of cell extracts revealed that in these experiments the two inhibitor proteins were expressed at approximately the same level (data not shown). However, whereas RraA and RraB had quantitatively similar effects on the ability of RNase E to cleave *rne* mRNA, their effects on the endonucleolytic cleavage of pM1 were very different. Specifically, in cells expressing RraA, uncleaved pM1 accounted for 30% of the total signal intensity, which is a 10-fold increase over the control, while RraB expression resulted in only a 1.5-fold increase in pM1 abundance (from 3% to 8%, Fig. 2D). Differential effects of RraA and RraB on the processing of asn-tRNA were similarly evident: RraB had a small, albeit reproducible effect on asn-tRNA cleavage, while the effect of RraA on asn-tRNA processing was prominent (Fig. 2E). In KSL2009 cells, which express the catalytic domain (amino acids 1–498) of RNase E under the arabinose-inducible promoter, RraB had no effect on the abundance of asn-tRNA.

Taken together, the above results suggest that RNase E cleavage of the pM1 and asn-tRNA transcripts is differentially affected by RraA and RraB. Genome-wide analysis of RNA abundance at single gene resolution was carried out to further examine the effect of RraA and RraB on RNA abundance on a global scale. Relative RNA levels in the presence or absence of each inhibitor were determined by two-colour hybridization to DNA microarrays containing 4405 known and predicted *E. coli* ORFs (Blattner *et al*., 1997). In these experiments the effect of RraA or RraB was compared with the consequence of RNase E depletion by arabinose withdrawal (Fig. 3A). Transcripts exhibiting the most dramatic increase ($>$ threefold) were individually clustered and are shown in Fig. 3B–E.

The steady-state level of 792 transcripts increased by at lease twofold upon expression of either RraA or RraB. In particular, RraA uniquely affected the steady-state level of 371 transcripts, while RraB altered the abundance of a separate set of 85 transcripts. An additional 127 RNAs accumulated to a greater degree during adventitious expression of either RraA or RraB; however, their abundance was not affected by RNase E depletion alone. Thus, the microarray analyses reveal that instead of simply acting as general inhibitors of RNase E, RraA and RraB specifically modulate RNA decay and therefore affect the intracellular levels of distinct sets of transcripts.

RraA and RraB had a marginal effect on transcript abundance in cells expressing the catalytic domain of RNase E (strain KSL2009) rather than the full-length protein (Fig. 3A), implying that the CTH of RNase E is required for these effects. Consistent with the notion that an elevated level of RraA and RraB is important for the inhibition of RNase E activity, deletion of one or both of these genes reduced the abundance of small sets of transcripts (data not shown).

Physical basis for the interaction between RraB and RNase E

What is the molecular basis for the ability of the RraB protein to affect RNase E cleavages? The possibility that purified RraB, like RraA, interacts directly with RNase E was addressed by surface plasmon resonance analysis on a BIACORE® 3000 instrument. Binding of RraB to the purified RNase E immobilized on the CM5 chip was detected as an increase in response units (RU). An equilibrium dissociation constant (K_D) of 28.2 μM was calculated by steady-state analysis (Fig. 4). This value is

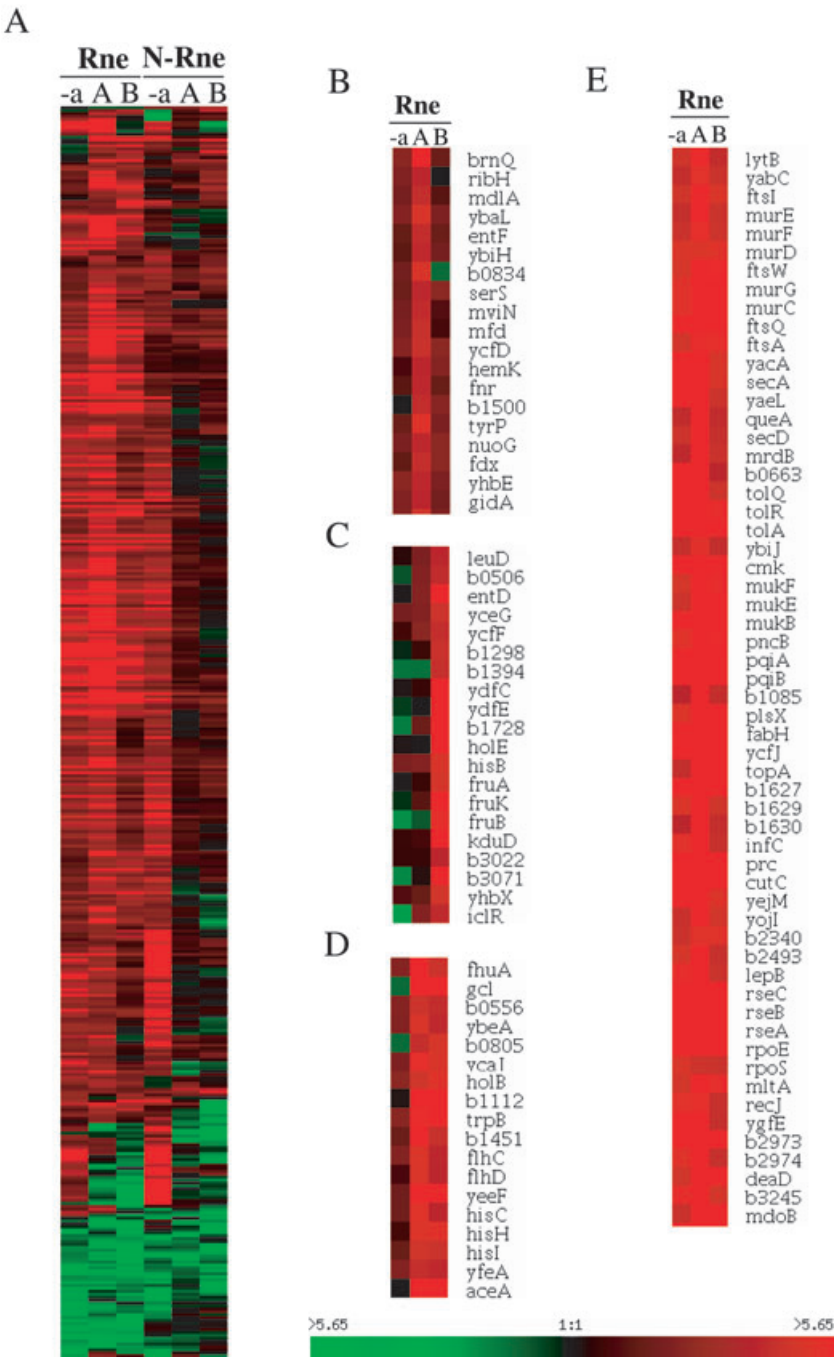

Fig. 3. Effect of RraB and RraA expression on the *E. coli* transcript profile.
A. Gene clusters whose relative mRNA levels were twofold or more changed in at least two out of four slides. Cy-5-labelled cDNAs were synthesized with RNA samples taken from strains: **–a**, KSL2000 plus pTrc99A (Rne) or KSL2009 plus pTrc99A (N-Rne) followed by withdrawal of arabinose for 1.5 h; **A**, KSL2000 plus pTrc-RraA or KSL2009 plus pTrc-RraA; **B**, KSL2000 plus pTrc-RraB or KSL2009 plus pTrc-RraB. RNA samples from KSL2000 plus pTrc99A (Rne) or KSL2009 plus pTrc99A (N-Rne) grown in the presence of 0.1% arabinose were labelled with Cy-3 and comparisons between paired cultures were done directly.
B. Cluster of genes whose transcript abundance was at least threefold increased when RraA is overexpressed in strain KSL2000.
C. Cluster of genes whose transcript abundance was at least threefold increased when RraB is overexpressed in strain KSL2000.
D. Cluster of genes whose transcript abundance was at least threefold increased when RraA is overexpressed or RraB is overexpressed in strain KSL2000.
E. Cluster of genes whose transcript abundance was at least threefold increased when RNase E is depleted or RraA is overexpressed or RraB is overexpressed in strain KSL2000.

statistically indistinguishable from the K_D of 26 μM determined earlier for the interaction of RraA with full-length RNase E (Lee *et al*., 2003). Binding of the purified RNase E catalytic domain (amino acids 1–498) to RraB could not be detected by surface plasmon resonance.

We further tested the *in vitro* inhibitory effect of RraA and RraB on purified full-length RNase E or on the catalytic domain only. p23 RNA is a truncated pM1 RNA that is processed by RNase E to a product termed 23 RNA (Kim *et al*., 1996). Addition of RraA *in vitro* resulted in a greater degree of inhibition than RraB throughout the concentration range tested. For example, at a 40-fold excess of inhibitory protein/RNase E, RraB resulted in 23% inhibition of p23 RNA processing over the control, whereas RraA inhibited processing by 45% (Fig. 5). RraB did not inhibit the processing of p23 by the purified N-terminal domain of RNase E. In contrast, RraA inhibited the processing of p23 by the N-terminal domain, albeit to a lesser extent than what was observed for the full-length protein.

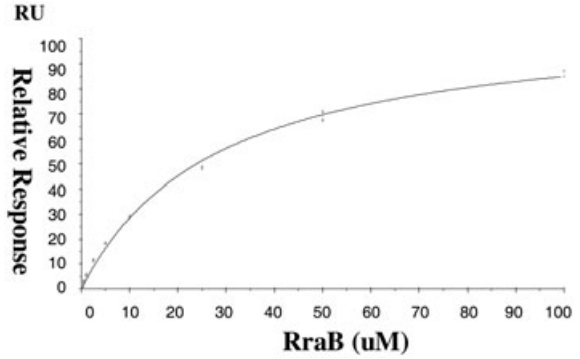

Fig. 4. RraB binds RNase E *in vitro.* The relative response, obtained by subtracting the online reference flow cell signal from the real signal, were plotted against concentration of RraB and fitted with a steady-state model. The experimental R_{max} was 109 RU and chi^2 was 2.99.

RraA and RraB interact differently with the CTH domain of RNase E

The differential effect of RraA and RraB on the catalytic activity of RNase E suggested that the mode of interaction of the two inhibitors with the enzyme may be distinct. The contribution of the various domains of RNase E to the binding of RraA or RraB was evaluated *in vivo* by co-precipitation analysis using a set of RNase E truncation mutants. Carpousis and coworkers constructed a series of isogenic strains in which the chromosomal *rne* gene was replaced by mutant alleles containing various C-terminal deletions (Leroy *et al*., 2002). For our analysis, RraB was fused to a 21-amino-acid extension (Biotag), which encodes a peptide substrate of the *E. coli* biotin holoenzyme synthetase (BirA; Schatz, 1993). While fusion of the Biotag peptide at the C-terminus destabilized the protein and gave no detectable expression, fusion at the N-terminus did not impact the steady-state accumulation of RraB relative to unfused protein (data not shown). Furthermore, no significant change in solubility or localization of RraB after biotinylation was observed. Expression of the Biotag–RraB fusion protein gave the same phenotypes as unmodified RraB, including increased DsbC accumulation and higher β-galactosidase activity expressed from the chromosomal *rne–lacZ* fusion (data not shown).

Biotinylated RraB synthesized in the AC series of RNase E C-terminal truncation mutants (Leroy *et al*., 2002) was precipitated with streptavidin beads and the presence of RNase E in the precipitate was detected by Western blot analysis using an antibody that recognizes the N-terminal domain. As expected, full-length RNase E was readily observed in the precipitate from cells expressing Biotag–RraB (Fig. 6B, first lane). Pretreatment of cell lysate with RNase A or Benzonase® nuclease (Novagen, WI) did not affect the co-precipitation of RNase E, indicating that nucleic acids are not involved in the ability of these two proteins to interact. No RNase E band was detected in cells expressing the Rne131 protein lacking the whole CTH (amino acids 585–1061) or in strain CJ1825/BZ99 expressing RNase E amino acids 1–602 (data not shown). Similarly, the RneΔ14 protein lacking amino acids 636–845 was not co-precipitated with the biotinylated RraB whereas RNase E mutant proteins lacking amino acids 603–693 and 728–845 gave a clear signal. This analysis suggests that the region between amino acids 694–727 is important for the binding of RraB to RNase E.

A similar experiment was performed using an RraA–Biotag fusion (Lee *et al*., 2003) and the results are presented in Fig. 6C. Interaction between RraA and RNase E was detected for all truncation mutants except for Rne131 protein (RneΔ585-1061). As seen in Fig. 5, RraA at a large molar excess inhibits the catalytic activity of the

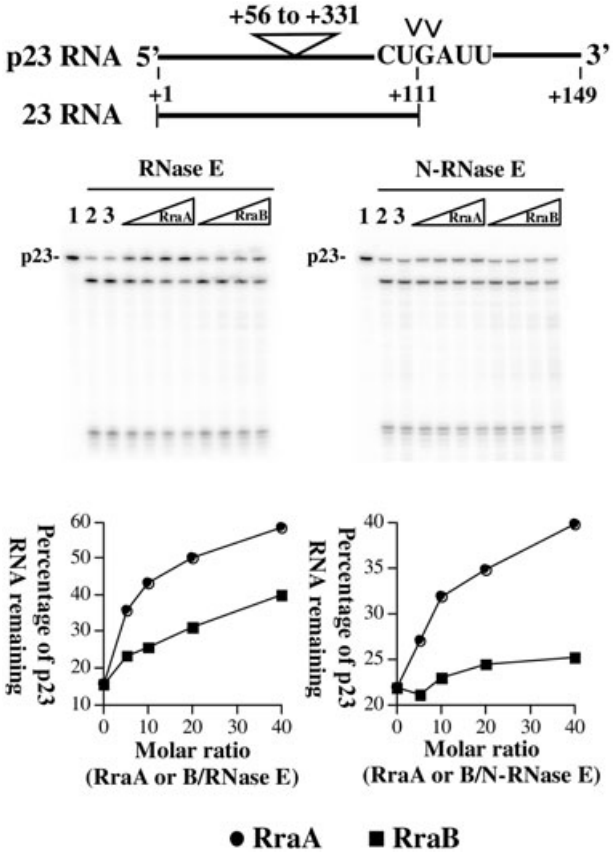

Fig. 5. RraB inhibits the *in vitro* cleavage of p23 RNA. Two picomoles of internally labelled p23 RNA were incubated with BSA only (**1**), RNase E or N-RNase E only (**2**,**3**), or 100 ng of RNase E or 200 ng of N-RNase E with varying concentrations of RraA or RraB in 20 μl of 1× cleavage buffer at 37°C for 30 min for RNase E, or for 90 min for N-RNase E or BSA only controls. The percentage of uncleaved pM1 in the gel was quantified using a Molecular Dynamics Phosphoimager and plotted as a function of the molar ratio of RraA/RNase E or RraB/RNase E in the assay.

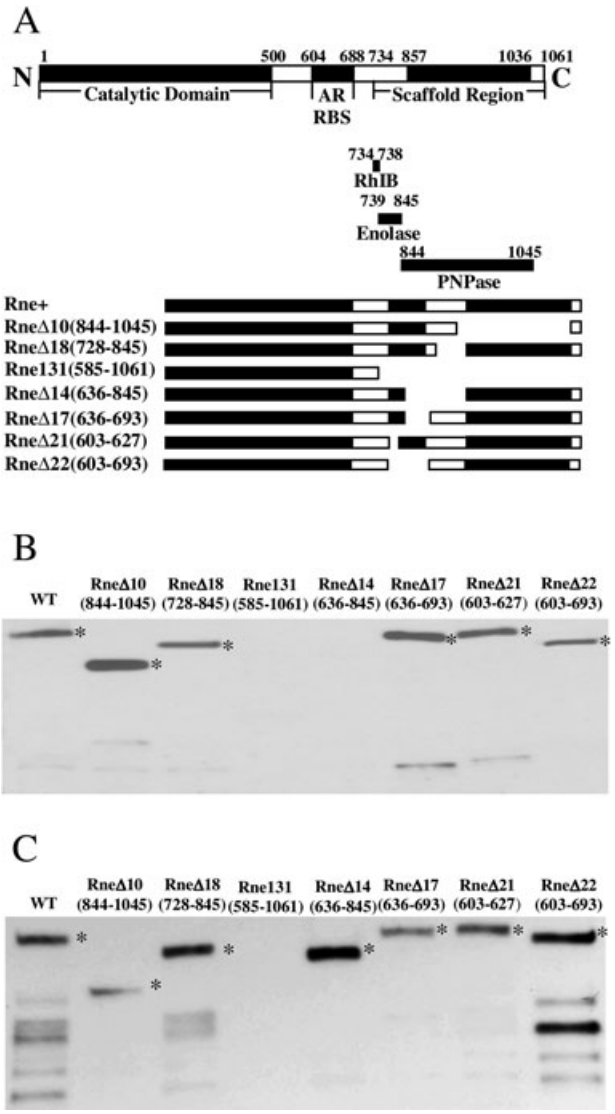

Fig. 6. Mapping the binding site of RraB and RraA on RNase E by co-precipitation analysis.
A. Schematic illustration of the structure of wild-type and truncated RNase E, adapted from Vanzo *et al.* (1998) and Leroy *et al.* (2002).
B. Western blot analysis of proteins co-precipitated with *in vivo* synthesized Biotag–RraB. The same amount of cell lysate protein was used in each co-precipitation. Asterisks (*) indicate the expected electrophoretic migration of the RNase E truncated mutant proteins in the absence of proteolytic degradation. WT, wild-type.
C. The same as above except that RraA–Biotag was used for the co-precipitation analysis.

RNase E NTH *in vitro* but the interaction between the two proteins is weak and shows a K_D in excess of 200 μM (Lee *et al.*, 2003). Thus, while it appears that RraA requires the CTH of RNase E for high affinity binding, we could not map the interaction of the two proteins to a single contiguous epitope. This is in contrast to RraB and all the major degradosome components which bind to defined continuous epitopes in the CTH.

Binding of inhibitors affects the degradosome composition

The fact that RraA and RraB interact with the scaffold region of RNase E at different locations led us to speculate that these two inhibitors might differentially affect the binding of other proteins to the CTH. To address this question, we took advantage of a recently developed affinity purification system for the analysis of protein complexes in *E. coli* (Butland *et al.*, 2005). In strain DY330 *rne-SPA,* the chromosomal *rne* gene had been fused to a DNA cassette that encodes a carboxyl-terminal sequential peptide affinity (SPA) tag. The SPA tag is composed of a 3× FLAG tag and a calmodulin-binding peptide (CBP) separated by a tobacco etch virus (TEV) protease cleavage site. The tagged RNase E was used as the bait to purify its interacting proteins by sequential affinity purification. The integrity and expression level of RNase E in the tagged strain are not affected as judged by Western blot analysis (data not shown).

The components of purified degradosomes were resolved by SDS-PAGE and visualized by colloidal blue staining (Fig. 7). To compare the relative abundance of individual degradosome components, protein samples loaded on each lane were normalized to the same amount of RNase E. The region of gel containing each of the detected bands was individually excised, proteolytically digested, and subjected to mass spectrometry analysis. As seen in Fig. 7, overexpression of RraA or RraB had a dramatic effect on the degradosome composition, most strikingly on the abundance of RNase E-bound PNPase. In degradosomes purified from control cells without RraA or RraB overexpression, the molar ratios of the major protein components to RNase E were as follows: PNPase, 5.4; RhlB, 2; enolase, 1.3. For clarity, all the above ratios were calculated based on relative polypeptide amounts without taking into account the oligomeric states of the respective proteins. The relative abundance we determined for these degradosome components in our experiments is comparable to those reported earlier by others (Py *et al.*, 1996; Coburn *et al.*, 1999). By contrast, in degradosomes isolated from cells expressing RraA, the ratios of PNPase, RhlB and enolase to RNase E were substantially lower, namely 0.7, 0.3 and 0.1 respectively. Similarly, in cells expressing RraB the ratios of RNase E-bound PNPase, RhlB and enolase dropped to 1.1, 0.9 and 0.6 respectively. Interestingly, RNase E from cells expressing RraA was found associated with markedly less RhlB compared with cells expressing RraB (RhlB to RNase E ratio of 0.3 versus 0.9). It is also noteworthy that expression of RraB, but not RraA, resulted in a moderate increase in RNase E-associated amounts of two non-stoichiometric components of degradosomes: DnaK and CsdA (DeaD).

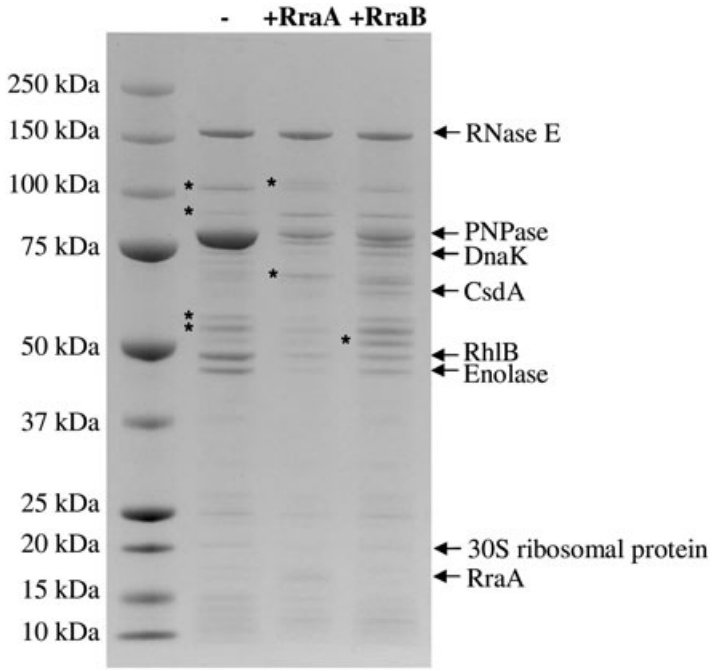

Fig. 7. RraA and RraB differently affect the composition of degradosomes. Purified degradosomes with and without overproduction of RraA or RraB were separated by SDS-PAGE and visualized by colloidal blue staining. The identities of protein bands were confirmed by mass spectrometry. Bands denoted with an asterisk correspond to RNase E degradation products.

Discussion

RraB was isolated genetically as a result of its ability to facilitate disulphide bond isomerization in the periplasmic space of *E. coli*, the same phenotype that had led to the earlier isolation of the prototypical RNase E inhibitor RraA (Lee *et al*., 2003). In a manner analogous to RraA, RraB stabilized the *dsbC* transcript, resulting in accumulation of the disulphide isomerase, DsbC. Both the RraA and RraB proteins inhibited endoribonucleolytic cleavage of the 5′ UTR of *rne* transcripts strongly enough to override the autoregulation of *rne* that normally maintains the level of the enzyme within a narrow range (Fig. 2). Genome-wide analysis of mRNA abundance by DNA microarrays revealed that the abundance of 18% of all *E. coli* transcripts (corresponding to 792 out of 4405 known and predicted ORFs, excluding small RNAs, Fig. 3) were affected by twofold or more when either RraA or RraB is expressed. Strikingly, however, not all RNAs were affected equally by both inhibitors. For example, the steady-state levels of pM1 and asn-tRNAs were each increased by about fivefold in cells expressing RraA, whereas expression of RraB had a marginal effect (Fig. 2). At a global scale, the microarray data established that while a large set of transcripts is affected similarly by either inhibitor protein, other equally large sets of transcripts are stabilized exclusively by RraA or by RraB. In particular, 336 transcripts corresponding to 7.6% of the transcriptome were stabilized equally by either protein inhibitor, 371 transcripts (8.4%) were affected uniquely by the expression of RraA and 85 transcripts (1.9%) were stabilized only by RraB. These results clearly demonstrate that the two inhibitor proteins exert a differential effect on the ability of RNA processing machinery to cleave various mRNAs, in turn giving rise to distinct transcript profiles.

What is the molecular basis for the selective effect of RraA and RraB on specific RNAs? Neither the crystal structure of RraA (Monzingo *et al*., 2003) nor the solution structure of the *Vibrio cholerae* RraB homologue, VC0424, contain putative nucleotide binding sites (Ramelot *et al*., 2003). Not surprisingly, RraA and RraB do not appear to interact directly with substrate RNAs (Lee *et al*., 2003; K.S. and S.N.C., data not shown). Instead, inhibition of RNA cleavage results from the direct interaction of the two proteins with RNase E. RraA and RraB exhibit nearly identical affinities for RNase E, with K_D values determined by surface plasmon resonance spectroscopy in the micromolar range. Similar weak binding affinities have been measured for other proteins that modulate the specificity of macromoloceluar machines. Examples include the binding of the adaptor protein SspB with ClpX (Wah *et al*., 2002) and the interaction between the active forms of ClpB and DnaK (K_D = 17 mM, Schlee *et al*., 2004).

Co-precipitation analysis using a set of RNase E mutants containing deletions in the CTH (Leroy *et al*., 2002) revealed that RraA and RraB interact with the enzyme in distinct ways. Even though RraA and RraB have a low pI they do not bind to the positively charged arginine-rich motif of RNase E (amino acids 604–688). Amino acids 694–727 were required for the binding of RraB to RNase E, similar to the major degradosome

components which bind to specific, continuous regions within the CTH (Py *et al*., 1994; 1996; Miczak *et al*., 1996; Vanzo *et al*., 1998; Coburn *et al*., 1999). This region partially overlaps a stretch of amino acids extending from position 685–712 which is predicted to form half of a putative coiled-coil that may be important for binding of the enzyme to structured RNAs (Callaghan *et al*., 2004). As expected, the endonucleolytic activity of the N-terminal catalytic domain which lacks the CTH region was unaffected by RraB, even when present at a large stoichiometric excess. In contrast, RraA inhibited the endonuclease activity of the N-terminal catalytic domain *in vitro*, albeit more weakly compared with the inhibition of the full-length RNase E (Fig. 5). Although this inhibitory effect strongly suggests a physical interaction between the two proteins, we could not detect the formation of a protein complex using surface plasmon resonance analysis, presumably because of the low binding affinity.

On the basis of these results we propose that the distinct mode of interaction of the two inhibitor proteins with RNase E is responsible for the selective stabilization of different sets of transcripts. The selective stabilization of some transcripts but not others is likely to be related to the way in which RraA and RraB mediate the remodelling of the degradosome. The two inhibitors had a similar effect on the amount of some degradosome components but reduced the level of other components in a distinct manner that was specific to each of the two proteins. *E. coli* degradosomes contain an excess of PNPase per RNase E polypeptide chain (Py *et al*., 1996; Coburn *et al*., 1999). However, in degradosomes isolated from cells expressing RraA or RraB, PNPase and RNase E were present in nearly equal amounts. On the other hand, RraA reduced the amount of RhlB and enolase associated with RNase E by sevenfold and 13-fold respectively, whereas RraB led to only a twofold reduction for both degradosome components. As a result of these effects, the stoichiometry of PNPase to RhlB and enolase bound to RNase E is different for control *E. coli*, for cells expressing RraA and for cells expressing RraB. Recently, Lin-Chao and coworkers (Lin and Lin-Chao, 2005) reported that PNPase and the RhlB helicase form an RNA-degrading complex independently of the attachment of both proteins to RNase E. By changing the composition of the degradosome, RraA and RraB may also be exerting an indirect effect on the amount of free, i.e. not RNase E-bound, PNPase and RhlB, in turn affecting other RNA-degrading complexes.

In addition to changes in the amount of PNPase, RhlB and enolase bound to RNase E, RraB gave rise to degradosomes that contained the non-canonical components DnaK and CsdA. Such an effect was not observed in degradosomes isolated from cells expressing RraA. The chaperone protein DnaK, which normally is present in degradosomes in small amounts (Miczak *et al*., 1996), has been found to increase significantly under certain stress conditions such as low temperature, RNase E overexpression, or in cells lacking PNPase (Regonesi *et al*., 2005). CsdA, was previously found associated with the RNA degradation machinery only under cold-shock conditions (Prud'homme-Genereux *et al*., 2004).

Comparison of the microarray data reported here with the genomic scale RNA stability data of Bernstein *et al*. (2002) did not reveal any substantial difference between the $t_{1/2}$ of transcripts that are affected by RraA and those affected by RraB. We also failed to identify a pattern in the length or in the function of the 371 RraA-specific or the 85 RraB-specific transcripts. Therefore more complex factors, possibly related to secondary structure considerations, might determine whether a particular RNA is stabilized through the action of RraA or RraB.

While homologues of RraA are widely distributed among archea, proteobacteria and plants, RraB homologues are found only in γ-proteobacteria – suggesting that these proteins may have a more specialized role in modulating RNA degradation. The existence of two proteins that exert a differential effect on RNA decay via their interactions with RNase E and degradosome remodelling, argues that modulation of RNA stability may be a mechanism for global control of transcript abundance in response to dynamic changes in the extracellular or intracellular environment. Along these lines, it is noteworthy that transcription of *rraA* from its own promoter is elevated upon entry of stationary phase in a *rpoS*-dependent manner and that the stability of *rraA* transcript is also dependent on RNase E activity (Zhao *et al*., 2006).

As both RraA and RraB were isolated as a consequence of their ability to stabilize the *dsbC* transcript, which encodes a protein mediator of disulphide bond rearrangements, we speculate that other proteins, and perhaps even nucleic acids that bind to RNase E and selectively affect the stability of sets of transcripts with different features, may be discovered by the application of alternative genetic screens.

Experimental procedures

Strains and plasmids

The strains and plasmids used in this work are listed in Table 1. The *rraB* null strain JG002 was constructed using the chromosomal gene inactivation method describe by Datsenko and Wanner (2000). The *rraA rraB* double null strain JG004 was constructed by transducing the allele into strain JQ004 with P1 phage.

Plasmid pDW363-RraB encoding a Biotag–RraB fusion was constructed by cloning the *rraB* gene into the XhoI-BamHI site of vector pDW363 (Tsao *et al*., 1996). The

Table 1. Strains and plasmids.

Strain/plasmid	Description	Reference or source
JCB570	MC1000, *phoR zih12*::*Tn10*	Bardwell *et al.* (1991)
JQ004	JCB570, *rraA*	Lee *et al.* (2003)
JG002	JCB570, *rraB*	This work
JG004	JCB570, *rraA rraB*	This work
MC1061	*araD39* Δ(*ara,leu*)*7697* Δ*lacX74 galU*$^-$ *galK*$^-$ *hsr*$^-$*hsm*$^+$*strA*	Casadaban and Cohen (1980)
CJ1825	MC1061 (λ*ez1)*	Jain *et al.* (2002)
CJ1825/BZ99	MC1061, *rne(1-602)* (λ*ez1)*	C. Jain
N3433	*lacZ43, relA, spoT, thi-1*	Goldblum and Apririon (1981)
KSL2000	*lacZ43, relA, spoT, thi-1, rne*::*cat*, *recA*::*Tn10* [pBAD-RNE]	Lee *et al.* (2002)
KSL2009	*lacZ43, relA, spoT, thi-1, rne*::*cat*, *recA*::*Tn10* [pBAD-NRNE]	Lee *et al.* (2002)
AC21	MC1061, *zce-726*::Tn*10*	Carpousis *et al.* (1994)
AC23	MC1061, zce-726::Tn10, *rne(ams)*	Vanzo *et al.* (1998)
AC24	AC23, *rneΔ10(aaΔ844-1045)*	Leroy *et al.* (2002)
AC26	AC23, *rneΔ18(aaΔ728-845)*	Leroy *et al.* (2002)
AC27	AC23, *rne131*	Leroy *et al.* (2002)
AC28	AC23, *rneΔ14(aaΔ636-845)*	Leroy *et al.* (2002)
AC29	AC23, *rneΔ17(aaΔ636-693)*	Leroy *et al.* (2002)
AC31	AC23, *rneΔ21(aaΔ603-627)*	Leroy *et al.* (2002)
AC32	AC23, *rneΔ22(aaΔ603-693)*	Leroy *et al.* (2002)
DY330 *rne-SPA*	W3110, *ΔlacU169 gal490 λcI857Δ(cro-bioA) rne-SPA*	Butland *et al.* (2005)
pBAD-stII-htPA	p15A *ori*, Cm^r, h-tPA with stII leader under PBAD	Qiu *et al.* (1998)
pTrc-RraA	ColE1 ori, Amp^r, *rraA* under *trc* promoter	Lee *et al.* (2003)
pTrc-RraB	ColE1 ori, Amp^r, *rraB* under *trc* promoter	This work
pTrc-RraA-Cm	ColE1 ori, Cm^r, *rraA* under *trc* promoter	This work
pDW363	pBR *ori*, Amp^r, *birA*	Tsao *et al.* (1996)
pDW363-RraA	pBR *ori*, Amp^r, *birA*, *rraA-biotag* under *trc* promoter	Lee *et al.* (2003)
pDW363-RraB	pBR *ori*, Amp^r, *birA*, *biotag-rraB* under *trc* promoter	This work
pDW363-DsbA	pBR *ori*, Amp^r, *birA*, *dsbA* under *trc* promoter	Lee *et al.* (2003)
pBAD-RNE	pSC101 *ori*, Km^r, *rne* under PBAD	Lee *et al.* (2003)
pBAD-NRNE	pSC101 *ori*, Km^r, *N-rne* under PBAD	Lee *et al.* (2003)
pLAC-RNE2	pSC101 *ori*, Amp^r, *rne* under PLAC	This work
pET28A-RraA	f1 ori, Kan^r, *rraA* under T7 *lac* promoter	Lee *et al.* (2003)
pET28A-RraB	f1 ori, Kan^r, *rraB* under T7 *lac* promoter	This work

chloramphenicol-resistant pTrc-RraA-Cm plasmid was constructed by inserting the Cm^r cassette into the Amp^r cassette of the pTrc-RraA plasmid (Lee *et al.*, 2003).

Fibrin plate assay

Fibrin solubilization by v-tPA was evaluated on fibrin plates prepared by mixing 80 ml of 3% agarose, 40 ml of 1× PBS containing 25 U of thrombin (Sigma, MO) and 40 ml of 1× PBS containing 400 mg of Fibrinogen (Sigma, MO). The same amount of total cell lysate protein was spotted on the plate and incubated at 37°C overnight. The size of the clearance is in proportion to the amount of active v-tPA in the sample.

Biochemical methods

Escherichia coli AC21 and derivatives were transformed with pDW363-rraA or pDW363-rraB and cultured in Luria–Bertani (LB) media containing 8 μg ml^{-1} of Biotin (Sigma, MO) at 37°C. Expression of biotinylated RraA or biotinylated RraB was initiated by addition of 1 mM of IPTG when the cell culture A_{600} reached ~0.4. Three hours after induction, the cells were harvested by centrifugation at 5000 rpm for 10 min and resuspended in 1/5 vol. of ice-cold NP-40 lysis buffer (150 mM sodium chloride, 1.0% NP-40, 50 mM Tris, pH 8.0). Cells were lysed by passing through a French press (2000 psi). The lysate was centrifuged for 15 min at 4°C to remove intact cells and cell debris and the protein concentration in the supernatant was determined. Aliquots containing 5 mg of protein were mixed with 100 μl of streptavidin bead slurry (Amersham Biosciences, Sweden) and the volume was adjusted to 800 μl. Following 1 h rotation at 4°C, samples were centrifuged at 6000 rpm for 5 min and the pellets were washed extensively five times with ice-cold NP-40 buffer. Finally, the streptavidin beads were recovered and proteins were released by boiling for 10 min in 2× SDS protein loading buffer [100 mM Tris-Cl (pH 6.8), 4% SDS, 200 mM β-mercaptoethanol]. The presence of RNase E was analysed by Western blotting using polyclonal anti-RNase E antiserum.

RNase E and N-RNase E used for the *in vitro* cleavage assay were purified from KSL2002 and KSL2003 respectively, as described previously (Lee *et al.*, 2002; 2003). Full-length RNase E used for surface plasmon resonance analysis was purified from BL21 harbouring pLAC-RNE3 and pTrc-RraA-Cm grown in LB media at 30°C. Coexpressing of RNase E and RraA was induced by adding 1 mM IPTG at A_{600} ~0.5. Cells were harvested after 2.5 h and lysed by French press. RNase E were affinity-purified using His·Bind® Kits (Novagen, WI) following the manufacture's protocol. The RNase E in the eluate was further purified by gel-filtration using a Superdex® 200 PC 3.2/30 column mounted on a SMART® system (Amersham Biosciences, Sweden). The peak fractions corresponding to RNase E

were concentrated by Centricon® YM-50 centrifugal filter devices (Millipore, MA).

RraA and RraB were purified from BL21 harbouring pET28A-RraA and pET28A-RraB respectively. Expression was induced with 1 mM IPTG for 3 h and the harvested cells were lysed using BugBuster® protein extract reagent (Novagen, WI). The clarified cell lysates were loaded onto a Mono Q HR 5/5 anion exchange column and proteins were eluted with 0–0.8 M NaCl gradient in 20 mM Tris·Cl buffer. Fractions containing RraA and RraB, respectively, were concentrated by Centricon® YM-3 centrifugal filter devices (Millipore, MA).

RNA methods

RNA protection assays were performed as previously described (Lee *et al*., 2003). The *dsbC* probe consisted of a sequence complementary to the +1 to +266 bp region of the *dsbC* transcript. The *rne* 5′ UTR probe was complementary to the −359 to +33 bp region of *rne* transcript. The band intensity from each sample was quantified using the ImageQuant® software.

To prepare total RNA from KSL2000 containing pTrc99A (no arabinose), cells were grown to mid-exponential phase in the presence of 0.1% arabinose, harvested, washed with LB medium two times, re-inoculated into LB medium containing no arabinose and finally grown at 37°C to an A_{600} ~0.2. At that point 0.5 mM IPTG was added, the cells were harvested 1.5 h later, and total RNA was prepared. Total RNA was isolated as described by Lin-Chao and Cohen (1991) and Northern blot analysis was performed as described previously (Lee *et al*., 2002). Oligonucleotide probes used were M1 (5′-GCTCTCTGTTGCACTGGTCG-3′) and $tRNA^{Asn}$ (5′-TACGGATTAACAGTCCGCCGTTCTACCGACTGAACTACAGA-3′) for pM1 RNA and $tRNA^{Asn}$ processing respectively.

p23 RNA transcript universally labelled with [a-^{32}P] UTP was synthesized as described previously (Kim *et al*., 1996; Lee *et al*., 2002) except that the purified p23 RNA was denatured at 75°C for 10 min in 2 mM Tris-HCl (pH 7.6) and renatured by cooling down slowly to 30°C for 30 min in a heating block. RNase E cleavage assays were performed as described previously (McDowall *et al*., 1995) except that proteins (RNase E and RraA or RraB) and p23 RNA were mixed in 1× cleavage buffer and pre-incubated on ice for 10 min before starting the cleavage reaction at 37°C.

Microarray procedures

Relative mRNA levels were determined by parallel two-colour hybridization to DNA microarrays (Schena *et al*., 1995) on glass slides containing 4405 known and predicted ORFs. Comparative measurements of transcript abundance were performed by directly determining the abundance of each gene's transcript relative to the wild-type sample, described by Khodursky *et al*. (2000). Analysis of data was performed using the software available at http://genome-www5.stanford.edu and http://rana.lbl.gov

Surface plasmon resonance analysis

Surface plasmon resonance analysis was performed at 25°C using a BIACORE® 3000 instrument (Biacore AB, Sweden). 2500 RU each of purified RNase E and bovine serum albumin were immobilized on different flow cells of a CM5 sensor chip using amine-coupling chemistry as described by the manufacturer (BIACORE® 3000 instrument handbook, Biacore AB). Purified RraB in the concentration range between 0 and 100 μM was injected at a constant flow rate of 30 μl min^{-1}.

SPA purification of degradosomes

The protocol was adapted from Butland *et al*. (2005) with modifications. One litre of *E. coli* cultures were grown in Terrific Broth (TB) at 32°C to an A_{600} ~0.6. Expression of RraA or RraB was induced with 1 mM IPTG for 3 h. Harvested cells were resuspended in lysis buffer (10 mM Tris·Cl pH 7.9, 100 mM NaCl, 0.2 mM EDTA, 0.5 mM DTT, 10% glycerol) with Complete® protease inhibitor cocktail (Roche, IN) and lysed by French press. Cell debris was removed by centrifugation at 20 000 *g* for 30 min. The whole cell extracts were first treated with Benzonase® nuclease (Novagen, CA) for 30 min and Triton X-100 was added to the final concentration of 0.1%. One hundred microlitres of Anti-FLAG M2 agarose beads (Sigma, MO) was added and incubated for 3 h with rotation. After extensive washing, the beads were resuspended in 200 μl of TEV buffer (50 mM Tris·Cl pH 7.9, 100 mM NaCl, 0.2 mM EDTA, 1 mM DTT, 0.1% Triton X-100) and digested with 5 μl of TEV protease overnight at 4°C. Following digestion, 400 μl of TEV buffer and 1.2 μl of 1 M $CaCl_2$ were added to the eluate and then incubated with 50 μl of calmodulin-sepharose beads (Amersham Biosciences, Sweden) for 3 h. After incubation, 400 μl of calmodulin binding buffer (10 mM Tris·Cl, 100 mM NaCl, 2 mM $CaCl_2$, 10 mM 2-mercaptoethanol, 0.1% Triton X-100, pH 7.9), followed by 100 μl of calmodulin wash buffer (10 mM Tris·Cl, 100 mM NaCl, 0.1 mM $CaCl_2$, 10 mM 2-mercaptoethanol, 0.1% Triton X-100, pH 7.9) were used to wash the beads. The purified complex proteins were recovered using 300 μl of calmodulin elution buffer and analysed by SDS-PAGE using NuPAGE® Novex 4–12% Bis-Tris gel (Invitrogen, CA). The gel was visualized by colloidal blue staining (Invitrogen, CA).

Mass spectrometry

The stained protein bands were cut out and in-gel digested with proteomic grade trypsin (Sigma, MO) at 37°C overnight. The tryptic peptide mixtures were subjected to Q-TOF Premier® mass spectrometer (Waters, MA) and the ProteinLynx (version 2.2) software was used to analyse each dataset for protein identification.

Acknowledgements

This work was supported by Grant NIH GM 55090 to G.G. and by Grant NIH GM 54158 to S.N.C. We are particularly grateful to A.J. Carpousis for his gift of the RNase E deletion mutant strain collection. We also thank A. Emily, J.G. Belasco, C. Jain and S.R Kushner for their gift of strains, Y. Lee for pSPd23 plasmid, S. Lin-Chao for polyclonal antibody to RNase E, C. Parrish for help with BIACORE analysis, K. Linse and M. Moini for help with mass spectrometry analysis.

References

Bardwell, J.C., McGovern, K., and Beckwith, J. (1991) Identification of a protein required for disulfide bond formation *in vivo*. *Cell* **67:** 581–589.

Bernstein, J.A., Khodursky, A.B., Lin, P.H., Lin-Chao, S., and Cohen, S.N. (2002) Global analysis of mRNA decay and abundance in *Escherichia coli* at single-gene resolution using two-color fluorescent DNA microarrays. *Proc Natl Acad Sci USA* **99:** 9697–9702.

Bernstein, J.A., Lin, P.H., Cohen, S.N., and Lin-Chao, S. (2004) Global analysis of *Escherichia coli* RNA degradosome function using DNA microarrays. *Proc Natl Acad Sci USA* **101:** 2758–2763.

Blattner, F.R., Plunkett, G., 3rd, Bloch, C.A., Perna, N.T., Burland, V., Riley, M., *et al.* (1997) The complete genome sequence of *Escherichia coli* K-12. *Science* **277:** 1453–1474.

Butland, G., Peregrin-Alvarez, J.M., Li, J., Yang, W., Yang, X., Canadien, V., *et al.* (2005) Interaction network containing conserved and essential protein complexes in *Escherichia coli*. *Nature* **433:** 531–537.

Callaghan, A.J., Aurikko, J.P., Ilag, L.L., Gunter Grossmann, J., Chandran, V., Kuhnel, K., *et al.* (2004) Studies of the RNA degradosome-organizing domain of the *Escherichia coli* ribonuclease RNase E. *J Mol Biol* **340:** 965–979.

Callaghan, A.J., Marcaida, M.J., Stead, J.A., McDowall, K.J., Scott, W.G., and Luisi, B.F. (2005) Structure of *Escherichia coli* RNase E catalytic domain and implications for RNA turnover. *Nature* **437:** 1187–1191.

Carpousis, A.J., Van Houwe, G., Ehretsmann, C., and Krisch, H.M. (1994) Copurification of *E. coli* RNAase E and PNPase: evidence for a specific association between two enzymes important in RNA processing and degradation. *Cell* **76:** 889–900.

Casadaban, M.J., and Cohen, S.N. (1980) Analysis of gene control signals by DNA fusion and cloning in *Escherichia coli*. *J Mol Biol* **138:** 179–207.

Coburn, G.A., and Mackie, G.A. (1999) Degradation of mRNA in *Escherichia coli*: an old problem with some new twists. *Prog Nucleic Acid Res Mol Biol* **62:** 55–108.

Coburn, G.A., Miao, X., Briant, D.J., and Mackie, G.A. (1999) Reconstitution of a minimal RNA degradosome demonstrates functional coordination between a 3′ exonuclease and a DEAD-box RNA helicase. *Genes Dev* **13:** 2594–2603.

Cohen, S.N., and McDowall, K.J. (1997) RNase E: still a wonderfully mysterious enzyme. *Mol Microbiol* **23:** 1099–1106.

Datsenko, K.A., and Wanner, B.L. (2000) One-step inactivation of chromosomal genes in *Escherichia coli* K-12 using PCR products. *Proc Natl Acad Sci USA* **97:** 6640–6645.

Ghora, B.K., and Apirion, D. (1978) Structural analysis and in vitro processing to p5 rRNA of a 9S RNA molecule isolated from an *rne* mutant of *E. coli*. *Cell* **15:** 1055–1066.

Goldblum, K., and Apririon, D. (1981) Inactivation of the ribonucleic acid-processing enzyme ribonuclease E blocks cell division. *J Bacteriol* **146:** 128–132.

Jain, C., and Belasco, J.G. (1995) RNase E autoregulates its synthesis by controlling the degradation rate of its own mRNA in *Escherichia coli*: unusual sensitivity of the *rne* transcript to RNase E activity. *Genes Dev* **9:** 84–96.

Jain, C., Deana, A., and Belasco, J.G. (2002) Consequences of RNase E scarcity in *Escherichia coli*. *Mol Microbiol* **43:** 1053–1064.

Jiang, X., and Belasco, J.G. (2004) Catalytic activation of multimeric RNase E and RNase G by 5′-monophosphorylated RNA. *Proc Natl Acad Sci USA* **101:** 9211–9216.

Khemici, V., and Carpousis, A.J. (2004) The RNA degradosome and poly(A) polymerase of *Escherichia coli* are required in vivo for the degradation of small mRNA decay intermediates containing REP-stabilizers. *Mol Microbiol* **51:** 777–790.

Khodursky, A.B., Peter, B.J., Cozzarelli, N.R., Botstein, D., Brown, P.O., and Yanofsky, C. (2000) DNA microarray analysis of gene expression in response to physiological and genetic changes that affect tryptophan metabolism in *Escherichia coli*. *Proc Natl Acad Sci USA* **97:** 12170–12175.

Kido, M., Yamanaka, K., Mitani, T., Niki, H., Ogura, T., and Hiraga, S. (1996) RNase E polypeptides lacking a carboxyl-terminal half suppress a mukB mutation in *Escherichia coli*. *J Bacteriol* **178:** 3917–3925.

Kim, S., Kim, H., Park, I., and Lee, Y. (1996) Mutational analysis of RNA structures and sequences postulated to affect 3′ processing of M1 RNA, the RNA component of *Escherichia coli* RNase P. *J Biol Chem* **271:** 19330–19337.

Kushner, S.R. (2002) mRNA decay in *Escherichia coli* comes of age. *J Bacteriol* **184:** 4658–4665; discussion 4657.

Lee, K., Bernstein, J.A., and Cohen, S.N. (2002) RNase G complementation of *rne* null mutation identifies functional interrelationships with RNase E in *Escherichia coli*. *Mol Microbiol* **43:** 1445–1456.

Lee, K., Zhan, X., Gao, J., Qiu, J., Feng, Y., Meganathan, R., *et al.* (2003) RraA. A protein inhibitor of RNase E activity that globally modulates RNA abundance in *E. coli*. *Cell* **114:** 623–634.

Leroy, A., Vanzo, N.F., Sousa, S., Dreyfus, M., and Carpousis, A.J. (2002) Function in *Escherichia coli* of the non-catalytic part of RNase E: role in the degradation of ribosome-free mRNA. *Mol Microbiol* **45:** 1231–1243.

Li, Z., and Deutscher, M.P. (2002) RNase E plays an essential role in the maturation of *Escherichia coli* tRNA precursors. *RNA* **8:** 97–109.

Li, Z., Pandit, S., and Deutscher, M.P. (1999) RNase G (CafA protein) and RNase E are both required for the 5′ maturation of 16S ribosomal RNA. *EMBO J* **18:** 2878–2885.

Lin, P.H., and Lin-Chao, S. (2005) RhlB helicase rather than enolase is the beta-subunit of the *Escherichia coli* polynucleotide phosphorylase (PNPase)-exoribonucleolytic complex. *Proc Natl Acad Sci USA* **102:** 16590–16595.

Lin-Chao, S., and Cohen, S.N. (1991) The rate of processing and degradation of antisense RNAI regulates the replication of ColE1-type plasmids in vivo. *Cell* **65:** 1233–1242.

Lin-Chao, S., Wei, C.L., and Lin, Y.T. (1999) RNase E is required for the maturation of ssrA RNA and normal ssrA RNA peptide-tagging activity. *Proc Natl Acad Sci USA* **96:** 12406–12411.

Lundberg, U., and Altman, S. (1995) Processing of the precursor to the catalytic RNA subunit of RNase P from *Escherichia coli*. *RNA* **1:** 327–334.

McDowall, K.J., and Cohen, S.N. (1996) The N-terminal domain of the *rne* gene product has RNase E activity and is non-overlapping with the arginine-rich RNA-binding site. *J Mol Biol* **255:** 349–355.

McDowall, K.J., Kaberdin, V.R., Wu, S.W., Cohen, S.N., and Lin-Chao, S. (1995) Site-specific RNase E cleavage of oligonucleotides and inhibition by stem-loops. *Nature* **374:** 287–290.

Mackie, G.A. (1998) Ribonuclease E is a 5′-end-dependent endonuclease. *Nature* **395:** 720–723.

Masse, E., Majdalani, N., and Gottesman, S. (2003) Regulatory roles for small RNAs in bacteria. *Curr Opin Microbiol* **6:** 120–124.

Miczak, A., Kaberdin, V.R., Wei, C.L., and Lin-Chao, S. (1996) Proteins associated with RNase E in a multicomponent ribonucleolytic complex. *Proc Natl Acad Sci USA* **93:** 3865–3869.

Miller, J.H. (1992) *A Short Course in Bacterial Genetics: A Laboratory Manual and Handbook for Escherichia coli and Related Bacteria*. Cold Spring Harbor, NY: Cold Spring Harbor Laboratory Press.

Monzingo, A.F., Gao, J., Qiu, J., Georgiou, G., and Robertus, J.D. (2003) The X-ray structure of *Escherichia coli* RraA (MenG), A protein inhibitor of RNA processing. *J Mol Biol* **332:** 1015–1024.

Mudd, E.A., and Higgins, C.F. (1993) *Escherichia coli* endoribonuclease RNase E: autoregulation of expression and site-specific cleavage of mRNA. *Mol Microbiol* **9:** 557–568.

Ow, M.C., Liu, Q., and Kushner, S.R. (2000) Analysis of mRNA decay and rRNA processing in *Escherichia coli* in the absence of RNase E-based degradosome assembly. *Mol Microbiol* **38:** 854–866.

Prud'homme-Genereux, A., Beran, R.K., Iost, I., Ramey, C.S., Mackie, G.A., and Simons, R.W. (2004) Physical and functional interactions among RNase E, polynucleotide phosphorylase and the cold-shock protein, CsdA: evidence for a 'cold shock degradosome'. *Mol Microbiol* **54:** 1409–1421.

Py, B., Causton, H., Mudd, E.A., and Higgins, C.F. (1994) A protein complex mediating mRNA degradation in *Escherichia coli*. *Mol Microbiol* **14:** 717–729.

Py, B., Higgins, C.F., Krisch, H.M., and Carpousis, A.J. (1996) A DEAD-box RNA helicase in the *Escherichia coli* RNA degradosome. *Nature* **381:** 169–172.

Qiu, J., Swartz, J.R., and Georgiou, G. (1998) Expression of active human tissue-type plasminogen activator in *Escherichia coli*. *Appl Environ Microbiol* **64:** 4891–4896.

Ramelot, T.A., Ni, S., Goldsmith-Fischman, S., Cort, J.R., Honig, B., and Kennedy, M.A. (2003) Solution structure of *Vibrio cholerae* protein VC0424: a variation of the ferredoxin-like fold. *Protein Sci* **12:** 1556–1561.

Regonesi, M.E., Del Favero, M., Basilico, F., Briani, F., Benazzi, L., Tortora, P., *et al.* (2005) Analysis of the *Escherichia coli* RNA degradosome composition by a proteomic approach. *Biochimie* **88:** 151–161.

Schatz, P.J. (1993) Use of peptide libraries to map the substrate specificity of a peptide-modifying enzyme: a 13 residue consensus peptide specifies biotinylation in *Escherichia coli*. *Biotechnology (NY)* **11:** 1138–1143.

Schena, M., Shalon, D., Davis, R.W., and Brown, P.O. (1995) Quantitative monitoring of gene expression patterns with a complementary DNA microarray. *Science* **270:** 467–470.

Schlee, S., Beinker, P., Akhrymuk, A., and Reinstein, J. (2004) A chaperone network for the resolubilization of protein aggregates: direct interaction of ClpB and DnaK. *J Mol Biol* **336:** 275–285.

Steege, D.A. (2000) Emerging features of mRNA decay in bacteria. *RNA* **6:** 1079–1090.

Taraseviciene, L., Bjork, G.R., and Uhlin, B.E. (1995) Evidence for an RNA binding region in the *Escherichia coli* processing endoribonuclease RNase E. *J Biol Chem* **270:** 26391–26398.

Tsao, K.L., DeBarbieri, B., Michel, H., and Waugh, D.S. (1996) A versatile plasmid expression vector for the production of biotinylated proteins by site-specific, enzymatic modification in *Escherichia coli*. *Gene* **169:** 59–64.

Vanzo, N.F., Li, Y.S., Py, B., Blum, E., Higgins, C.F., Raynal, L.C., *et al.* (1998) Ribonuclease E organizes the protein interactions in the *Escherichia coli* RNA degradosome. *Genes Dev* **12:** 2770–2781.

Wah, D.A., Levchenko, I., Baker, T.A., and Sauer, R.T. (2002) Characterization of a specificity factor for an AAA+ ATPase: assembly of SspB dimers with ssrA-tagged proteins and the ClpX hexamer. *Chem Biol* **9:** 1237–1245.

Zhan, X., Gao, J., Jain, C., Cieslewicz, M.J., Swartz, J.R., and Georgiou, G. (2004) Genetic analysis of disulfide isomerization in *Escherichia coli*: expression of DsbC is modulated by RNase E-dependent mRNA processing. *J Bacteriol* **186:** 654–660.

Zhao, M., Zhou, L., Kawarasaki, Y., and Georgiou, G. (2006) Regulation of RraA, a protein inhibitor of RNase E-mediated RNA decay. *J Bacteriol* **188:** 3257–3263.